Analysis of Urban Expansion and its Impact on Land Surface Temperature in Lome City (Togo) Using Remote Sensing and Gis

Komi A. Edokossi[1] Recep Bakis[2]

Abstract— Land surface temperature (LST) monitoring is being increasingly recognized due to the role it plays in environmental studies; and there is a strong interest in retrieval or measuring it from the space due to quickly retrieval methods and large study area covering.

In this paper, NDVI-based emissivity method was used for retrieving LST from Landsat 4 TM and Landsat 8 OLI/TIRS. This method walked through the computation of the At-sensor brightness temperature which was transformed into LST using the emissivity calculated from the proportion of vegetation (PV) deducted from NDVI. In addition, analysis of the land use/land cover (LULC) change and its impact on the LST in the study area, Lomé city (Togo), was carried out to investigate the relationship between the land cover types, NDVI and the LST.

The results showed LST variation over a period of time and based on land cover type i.e. high temperatures in fully built-up areas and low temperatures in the vegetated areas or water bodies. Furthermore, as the NDBI increases and the NDVI decreases, the LST increases. That means the higher biomass a land cover has, the lower the LST is. But the noticeable thing in this analysis is that the urban development between 1988 and 2018 has given an increase of minimum surface temperature (12.76 °C in 1988 against 22.76 °C in 2018).

Keywords--- Emissivity, Landsat, Land Surface Temperature, Brightness temperature, NDVI-based method

1 INTRODUCTION

Urbanization is the main type of land use/land cover change accross the world with a huge impact on climate and environment. Urban areas have generally high air temperature due probably to the reduction of its greenness and high solar radiation because of its high impervious surfces such as buildings, asphalt roads and others. In addition to those factors enumerated above, waste heat released from industries, transportation and houses create urban heat island (UHI), spots of heavy heat. And this has significant effects on all aspects of human life such as comfort, air pollution, energy management,...etc. Then there is a need to monitor the surface temperature in urban environment by retrieving and analysing this surface temperature periodically in order to assess conditions and make decision. However the traditional methods of retrieving the land surface temperature are very expensive and time-consuming mostly when covering a large study area.

According to [1], there is a growing awareness among environmental scientists that remote sensing technologies can and must play a role in providing the data needed to assess ecosystems conditions and to monitor change at all spatial scales. Thus, acquiring LST through remote sensing technologies becomes one of the significant methods nowadays, as LST is a key parameter in a changing climate [2].

Remote sensing and GIS integration has been widely applied and recognized by many of scientists and companies as an efective tool in detecting urban LST change [3]. With the development of the spatial technologies in this era, satellites remote sensing are very powerful in collecting data and turns them into valuable informations
for monitoring urban land processes. Some of the satellites' sensors are capable to record thermal data that is used to give average LST.

A number of methods for retrieving LST from space have been established. Among those methods, there are single-channel methods (mono-window algorithm or Qk&B algorithm, single channel algorithm or $SC^{JM\&S}$ proposed by Jiménez-Muñoz and Sobrino, 2003), two-channel methods or multi-channel algorithms (split-window method), classification-based emissivity method, NDVI-based emissivity methods, day/night temperature independent spectral indices (TISI) based methods, two-temperature methods, temperature emissivity separation methods (TES), ...etc. [4]

Most of scholars and scientists accross the world used those retrieval methods for measurements of LST from space. . Some examples are the effects of land use on LST in Netherlands by [5], in Dhaka Bangladesh by [6], in Addis Ababa City, Ethiopia

- *Komi A. Edokossi is currently pursuing doctorate degree program in Remote Sensing & GIS, Eskisehir Technical University, Eskisehir, Turkey. ametokomi@gmail.com, kaedokossi@eskisehir.edu.tr*
- *Prof. Dr. Recep Bakis is professor in the Faculty of Engineering, Eskisehir Technical University, Eskisehir, Turkey. rbakis@eskisehir.edu.tr*

by [7], and many others. [8], showed the capabilities of those techniques in studying and estimating the spatial distribution and intensities of geophysical parameters using Landsat 7 ETM+.

In Lomé, the capital city of Togo, LULC has changed drastically in lapse of time because of ownership house development and an unappropriate planning. This study aims at demonstrating integration of remote sensing and GIS in LST retrieving and investigating the relationship between the land cover change and this surface temperature variation. The importance of the study is to identify spatial factors affecting LST in urban areas. Understanding this spatial distribution and its impact factors allows to mitigate urban heat islands (UHI) effects and for sustainability in urban areas.

2 STUDY AREA

Situated on the west coast of Africa (mostly between latitudes 6° and 11°N, and longitudes 0° and 2°E),Togo (officially the Togolese Republic) has an area of 56,785 sq km, and is bounded on the North by Burkina Faso, on the East by Benin, on the South by the Gulf of Guinea, and on the West by Ghana, with a total boundary length of 1,703 km (1,058 mi), of which 56 km (35 mi) is coastline.

Lomé our study area, is the capital city of Togo. It is located 6.14 degree latitude North and 1.21 degree longitude East and it is situated at elevation 6 meters above sea level. November, 2010 census gave Togo a population of 6,191,155, more than double the total counted in the last census. Most of the population (62,3%) live in rural villages dedicated to agriculture or pastures while 37,7% in urban zones. Average population density is 109 hbts/km2. While the population of Lomé commune is 839.566 hbts with the average population density of 9305 hbts/km2 on 90 km2 ; the large Lomé has 1.5 million residents on an area of 333km2.

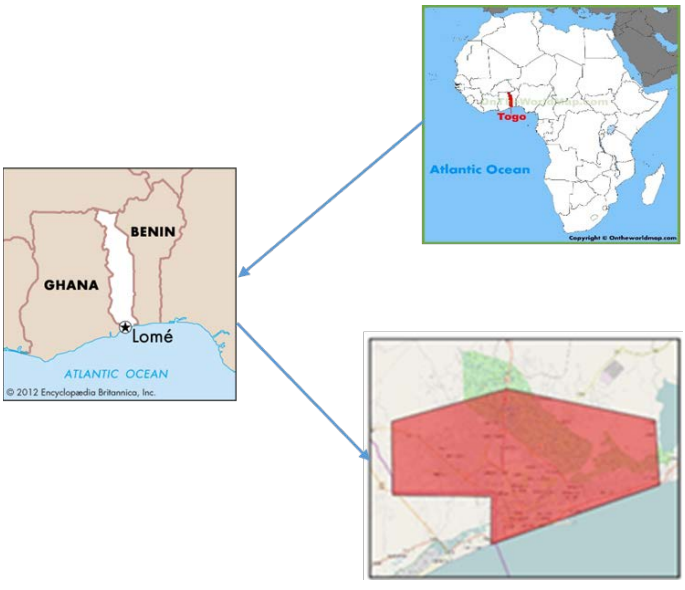

Fig. 1 Study area

3 MATERIALS AND METHODS

3.1 Materials

Landsat 4 TM and Landsat 8 OLI/TIRS were used as inputs data (http://earthexplorer.usgs.gov/).

Landsat 8 has two major instruments (OLI and TIR), at the 30m spatial resolution for the SWIR, visible and NIR, 100 m for the TIR (resampled to 30 m) and 15m for the panchromatic bands. The presence of double TIR bands in the Landsat 8 OLI/TIRS satellite in the atmospheric window (10-12µm) is the main advantage over previous Landsat series. ERDAS imagine 2014 was used for images processing and classification and ArcGIS 10.3 is used for the data computation and analysis.

TABLE I. LANDSAT DATA TYPES AND SPATIAL RESOLUTION

Data types	Spatial resolution	Acquisition date
Landsat 4 TM	30 m	12-02-1988
Landsat8 OLI/TIRS	30 m	05-01-2018

Source: https://landsat.usgs.gov

3.2 Methods

In this paper, the land surface temperature was retrieved from the thermal band; the digital numbers (DN) were first converted into radiance (spectral radiance) using the metadata file, next the thermal band data to the At-sensor brightness temperature (top of atmosphere brightness temperature) which was finally transformed into land surface temperature. But before obtaining this land surface temperature, NDVI-based emissivity method was applied to At-sensor brightness temperature. This method requires parameters such as, proportion of vegetation (PV) derived from calculated NDVI. With this method, the assumption is that surface is composed of soil and vegetation. And the variation of land surface emissivity is linearly dependent on the proportion of vegetation. The advantages of this method is its simplicity and suitable for various sensors with red/near infrared bands and thermal band and does not require accurate atmospheric correction. The flowchart of the study can be computed as follows:

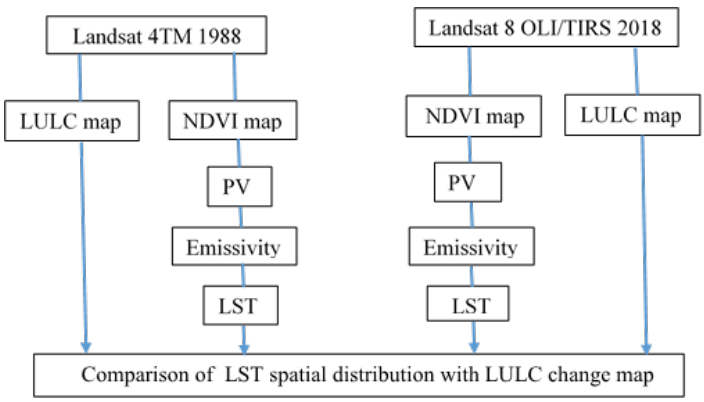

Fig. 2 Flowchart of the study

3.2.1 Top of atmosphere spectral radiance

As mentionned in the previous lines, first there was conversion of digital numbers of the thermal band into spectral radiance as follows:

- For TM4,

$$L\lambda = \frac{Lmax - Lmin}{Qcalmax - Qcalmin} * Qcal - Qcalmin + Lmin \quad (1)$$

Where, Lmax and Lmin are maximum and minimum spectral radiances, Qcalmax and Qcalmin are maximum and minimum quantized calibrated pixel value in DN, Qcal is the quantized calibrated pixel value in DN.

- For L8 OLI/TIRS, $L\lambda = MLQ_{cal} + AL$ (2)

$L\lambda$ is the spectral radiance and ML, AL and Qcal are the constants in the metedata of the image.

3.2.2 At sensor brightness temperature

After the conversion into spactral radiance, the TIR data were then converted to Brightness Temperature using the thermal constants in the metadata file.

$$TB = \frac{K_2}{Ln\ K_1/L\lambda + 1} - 273.15 \quad (3)$$

TB = At-sensor brightness temperature (℃), $L\lambda$ is the calculated spectral radiance, K1 and K2 are the constants in the metadata of the image.

3.2.3 Land surface emissivity calculation

At this step, the emissivity must be computed and applied to the At-sensor Brightness Temperature in order to calculate the temperature at final. But before computing this emissivity, the NDVI and proportion or fractional of vegetation (Pv or FVC) must be known since it is NDVI-based emissivity.This parameter can be measured directly or can be estimated through various available algorithms such as image classification-based method (Snyder et al, 1988), NDVI-based methods (NDVI-image based method with regression analysis by Van de Griend and Owe,1993; method based on the ratio of vegetation and bare ground proposed by Valor and Caselles, 1996; and NDVI threshold method intoduced by Sobrino and Raissouni, 2000).

- Image-based classification method which assigns emissivity value to each land use/land cover category, seems more appropriate and simple but the coeffi-cients *a* and *b* depend a lot of the study area and ones obtained from a study area cannot be applied to an-other study area.

$$\varepsilon = a + b \ln(NDVI) = 1.0094 + 0.047 \ln(NDVI) \quad (4)$$

- The ratio of vegetation and bare soil method supposes that the land surface is composed by soil and vegetation and requires some geometrical parameters a priori which makes the method utilization complex.

$$\varepsilon = \varepsilon_v P_v + \varepsilon_s(1 - P_v) + 4x \langle d\varepsilon \rangle x P_v x(1 - P_v) \quad (5)$$

Where, ε, ε_v and ε_s are the emissivities of ground, vegetation and bare soil respectively and $d\varepsilon$ is revised parameter averagely 0.01 and Pv is the percentage of vegetation :

$$PV = [(NDVI - [NDVI]_s)/([NDVI]_v - [NDVI]_s)] \quad (6)$$

- NDVI-based method with NDVI threshold seems to be simple and does not need accurate atmospheric correction. This method was used to compute emissivity in this study due to its simplicity. With this method, the land surface is supposed to be composed of soil and vegetation and the emissivity is linearly depends on the proportion of vegetation in a pixel. It distinguishes between soil pixels (NDVI < $NDVI_s$), full vegetation pixels (NDVI > $NDVI_v$) and mixed pixels of soil and vegetation ($NDVI_s$ < NDVI < $NDVI_v$).

$$\varepsilon = \begin{cases} a_\lambda + b_\lambda \rho_{red} & NDVI < NDVI_s \\ \varepsilon = \varepsilon_{s\lambda}(1 - FVC) + \varepsilon_{v\lambda} FVC + C_\lambda & NDVI_s < NDVI < NDVI_v \\ \varepsilon_{v\lambda} + C_i & NDVI > NDVI_v \end{cases} \quad (7)$$

ε_v and ε_s are vegetation and soil emissivity respectively, FVC is the proportion of vegetation; and *C* is a term that takes into account the cavity effect due to surface roughness (*C* = 0 for flat surfaces).

TABLE II. EMISSIVITY CONSTANTS (JIMENEZ-MUNOZ ET AL., 2014)

Emissivity	Band 10	Band 11
ε_v	0.987	0.989
ε_s	0.971	0.977

To calculate the emissivity for NDVI-based threshold method, the proportion of vegetation (PV) must be known and can be derived from NDVI.

- NDVI calculation

NDVI is an important indicator used to analyse the biomass or greenness of an area. As Weng et al., (2014) stated, estimating

NDVI is crucial since the quantity of vegetation is a parameter for surface temperature retrieval. The formula used for deriving the NDVI is as follows:

$$NDVI = (NIR - R)/(NIR + R) \quad (8)$$

NIR is for the near-infrared, R for the red bands.

- Proportion of vegetation cover

Spatial variation in the radiometric temperature of surfaces is related to variations of the soil water concentration vertically and surface greenness detailed by the proportion of vegetation. Hence, the formula as described in Wang et al., (2015) was used in deriving the proportion of vegetation cover (Pv) from the NDVI image and the formula is as follows:

$$PV[(NDVI - [NDVI]\_s)/([NDVI]\_v - [NDVI]\_s)]^2 \quad (9)$$

With NDVImin for bare soil and NDVImax for full vegetation.

3.2.4 Land surface temperature

Here is the formula to compute the final land surface temperature or emissivty-corrected land surface temperature:

$$LST = TB/(1 + (\lambda * TB/\rho)ln(\varepsilon)) \quad (10)$$

Where, LST is the land surface temperature in Celsius (°C),
TB is at-sensor brightness temperature (°C),
λ is the wavelength of emitted radiance (for which the peak response and the average of the limiting wavelength (λ=10.8μm for band 10 of Landsat 8 OLI/TIR),
ε is the calculated emissivity and

$$\rho = h\,C/\sigma = 1.438 \times [10]\text{^}(-2)\ mK$$

Where, σ is the Boltzmann constant (1.38 × 10−23 J/K), h is Planck's constant (6.626 × 10−34 J s), and C is the velocity of light (2.998 × 108 m/s).
These are the land surface temperature maps for 1988 and 2018 respectively.

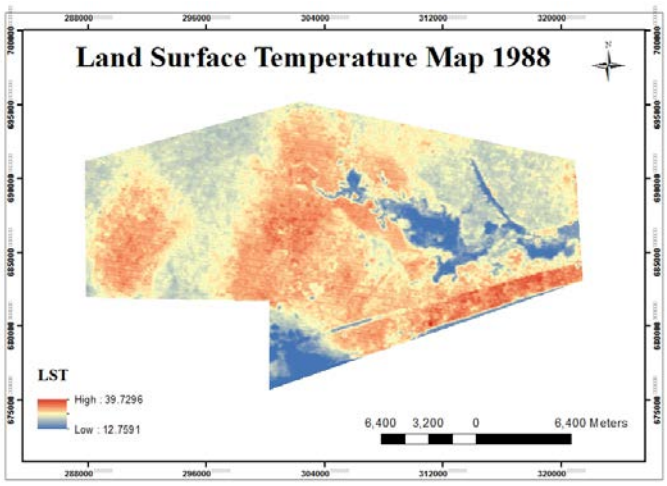

Fig. 3 LST map 1988

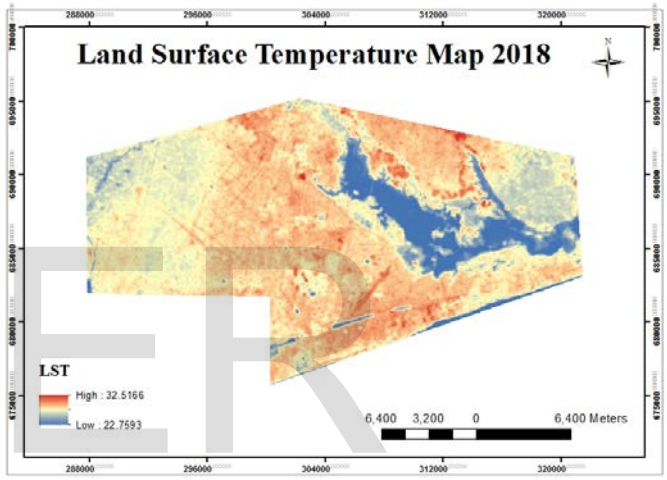

Fig. 4 LST map 2018

3.2.5 Land use/ land cover map generation for 1988 and 2018

To investigate if the land surface temperature values distribution depends on land cover types, land use/land cover maps for 1988 and 2018 were generated and analysis was carried out between the covers types and land surface temperature values. Unsupervised classification and recod method was used to get the final land use/land cover maps. The overall classification accuracy is 94% and 90% and the Kappa statistics is about 0.91 and 0.87 repectively for the year 2018 and 1988, which is widely over the normals. That means the classification is highly accurate. The land use/land cover are as follow:

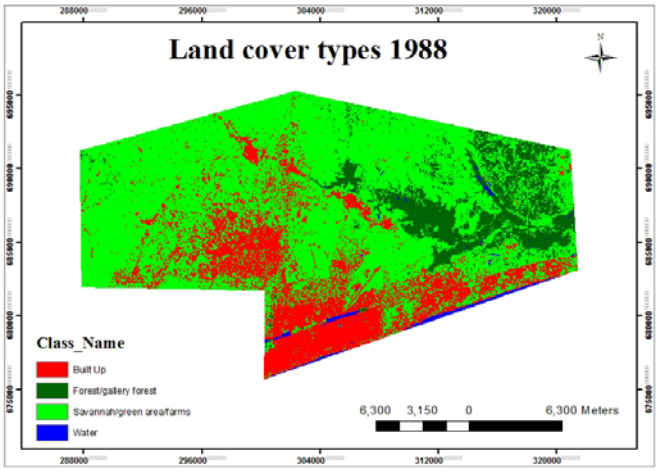

Fig. 5 LULC map 1988

NDBI	LST	NDVI
-0.06756628	18.4705297	0.53846157
-0.00675817	21.1146911	0.383544
0.05725037	23.2300202	0.31923859
0.11165762	25.2395829	0.2637021
0.15966402	26.9318462	0.21108859
0.20446999	28.0952773	0.16432102
0.24287511	29.3644748	0.11755345
0.28128024	30.5279058	0.06786291
0.31968536	33.595133	0.00940345
0.57251906	39.7295876	-0.08120872

(a)

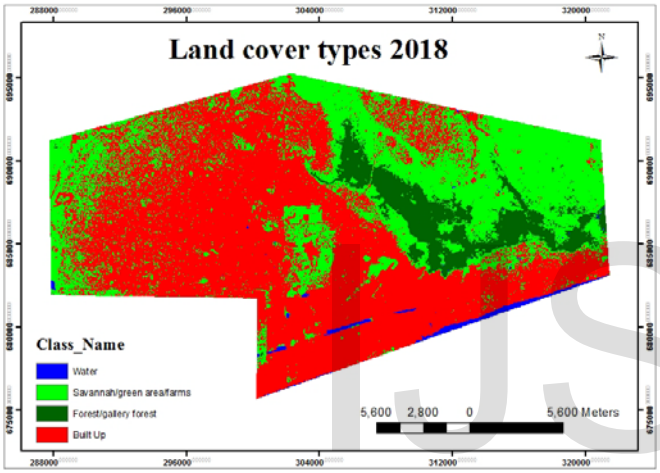

Fig. 6 LULC map 2018

NDBI	LST	NDVI
-0.15432616	23.983714	0.29785022
-0.12276199	25.0168485	0.23012085
-0.09119782	26.049983	0.20001891
-0.05963365	26.8535321	0.17367971
-0.03201501	27.4657599	0.14984901
-0.01031464	28.0014593	0.1285268
0.00546744	28.4606302	0.10845884
0.02124953	28.9198011	0.08713663
0.04294989	29.6085574	0.06205168
0.29349047	32.5166397	0.02317

(b)

3.2.6 NDBI and NDVI values generation from NDBI and NDVI maps for 1988 and 2018

NDBI and NDVI maps of the study area also were generated, reclassified in 10 classes and values recorded in the tables below also for the purpose to investigate the relationship betwen them.

4 RESULTS AND DISCUSSION

This part first, shows the spatial distribution of LST over the land use/land cover (LULC) types. The LST values are then retrieved from the LST maps overlaid on the LULC maps and recorded in the table table III with minimum, maximum and mean LST values for each LULC type as well as LULC type areas. And at last, the graphics highlighting the relations between the NDVI, NDBI and LST were done.

- LULC types and spatial distribution of LST values for 1988 and 2018

TABLE III. NDBI AND NDVI VALUES FOR 1988 (a) AND 2018 (b)

TABLE IV. LST DISTRIBUTION VALUES OVER LULC CLASSES IN 1988 AND 2018

	1988					
CLASS_NAME	ZONE CODE	COUNT	AREA (m2)	MIN (°C)	MAX (°C)	MEAN (°C)
Water	1	4557	4101300	12.76	32.53	23.53
Savannah/green area/farms	2	310596	279536400	13.22	38.25	28.80
Forest/gallery forest	3	58817	52935300	18.56	30.97	25.51
Built Up	4	104945	94450500	12.76	39.73	29.02
	2018					
CLASS_NAME	ZONE CODE	COUNT	AREA	MIN	MAX	MEAN
Water	1	4822	4339800	22.80	31.60	24.61
Savannah/green area/farms	2	158300	142470000	23.67	31.14	27.32
Forest/gallery forest	3	40626	36563400	22.76	28.69	24.04
Built Up	4	275167	247650300	24.38	32.52	28.18

From the table IV, it is clear that there has been a considerable change in LULC during the 30 years period. Urban built-up

areas have increased more than the double in the study area (104945 pixels in 1988 and 275167 pixels in 2018). Forest and farm lands have been decreased and converted into built up areas.

In order to understand the impacts of LULC change on LST, the values of the LST of each land cover type must be analyzed. For both periods according to the table, urban or built-up land exhibits the highest maximum surface temperature (39.72 °C in 1988 and 32.51 °C in 2018). This implies that urban development brings up surface temperature increase by replacing natural vegetation with non evaporating, non-transpiring surfaces such as stone, metal and concrete used in bulding, roads and transportation. The lowest minimum surface temperature observed in urban area in 1988 can be explained by the fact that the southwest part of the city is a residential area, one of the majors points the city originated, which was not covered by impervious or non transpiring surfaces and was always moist due to the fact that the soil is laid on water. The infrastructures development such roads and pavements was quasi-absent. That means more evaporation or transpiration. In 2018, all those areas have been developped. For that same date (1988), the highest minimum value for forest class could be due to pixel classification error. The differences in the maximum values between 1988 and 2018 could be due to the difference in the acquisition dates and times and atmospheric conditions probably. The 1988 image was taken on 12 february (dry season with forest fire occurrence) while the 2018 image on 05 january (period of harmattan in the region with coldness). The minimum surface temperature also raised from 12.76 °C in 1988 to 22.76 °C in 2018

- Relationship between LST-NDBI-NDVI for 1988 and 2018

In order to detect whether there is a relationship between NDBI, NDVI and the LST, graphics were drawn by pair of elements. The analysis showed that LST is related to NDVI values.

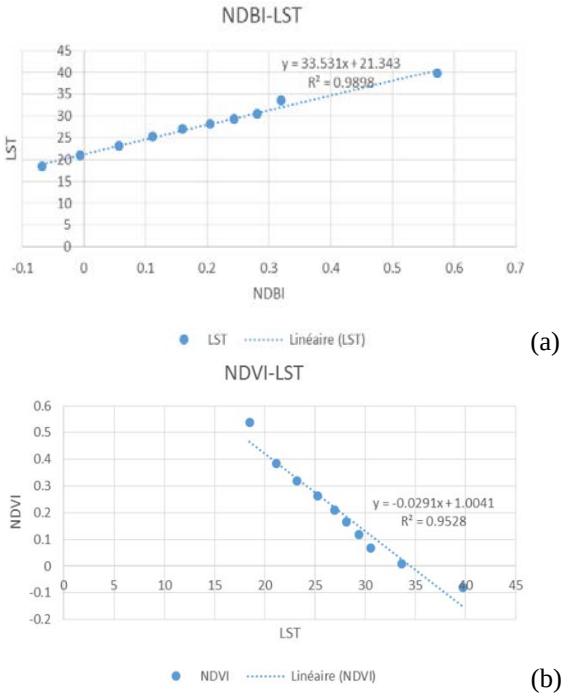

Fig. 7 Relationship between (a) NDBI-LST 1988 and (b) NDVI-LST 1988

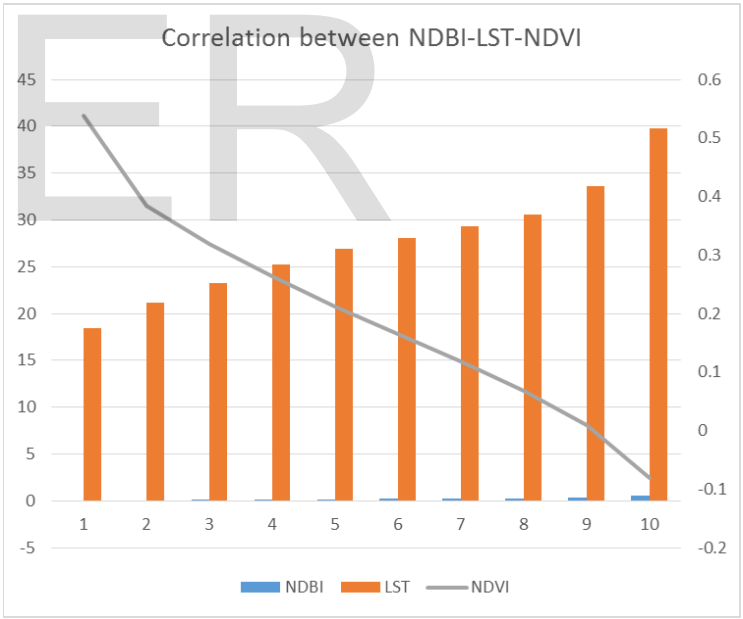

Fig. 8 Correlation between NDBI-LST-NDVI 1988

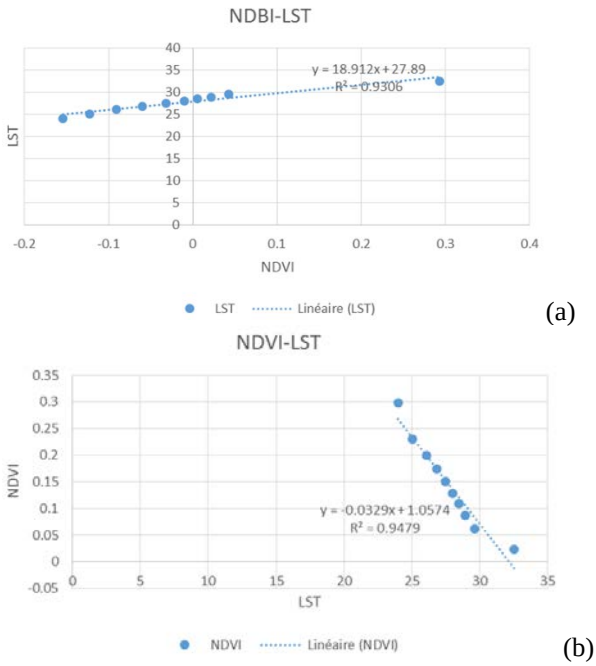

Fig. 9 Relationship between (a) NDBI-LST 2018 and (b) NDVI-LST 2018

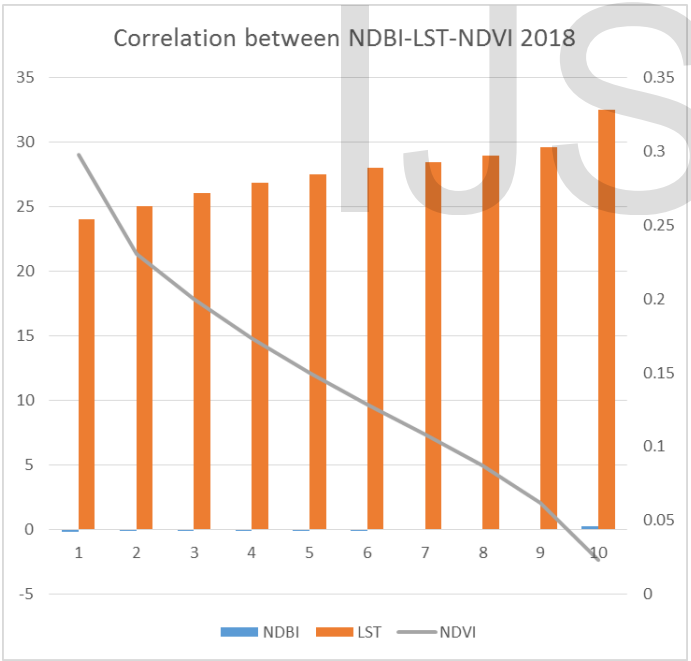

Fig. 10 Correlation between NDBI-LST-NDVI 2018

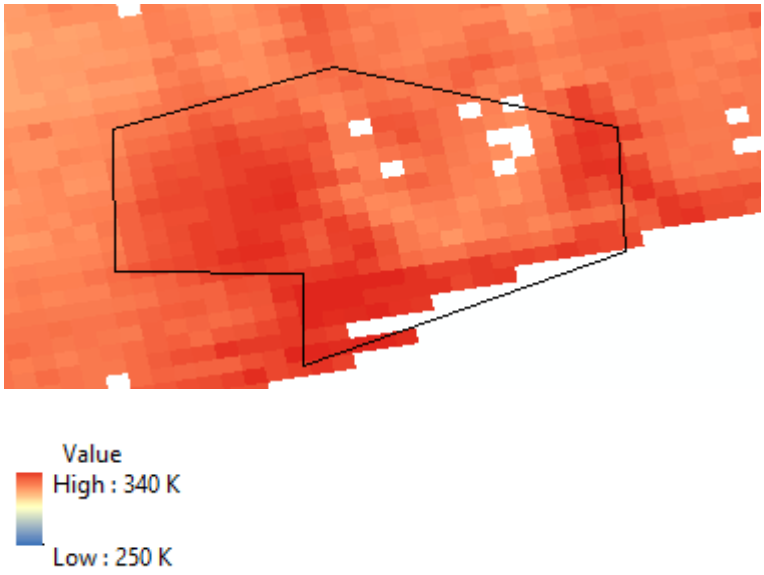

Fig. 11 MODIS/Terra LST/Emissivity 5-Min L2 Swath 1km V006 for 2018 (in ºK) Source: https://earthexplorer.usgs.gov/

The analysis of the graphics shows that as the NDBI increases, the LST also increases and as the NDVI decreases, the LST increases.That means the higher biomass a land cover has, the lower the LST is. Because of this relationship between LST and NDVI, changes land use/land cover have an indirect impact on LST through NDVI.

The most noticeable thing is that the minimum LST in the study area increased from 12.76 °C in 1988 to 22.76 °C in 2018 showing global the raising of the surface temperature. This surface temperature raising are the results of reduction in greenness or NDVI values, increase in land covers with high surface radiant and augmentation of heat release from industries, transportation and houses which are constantly growing.

- Validation of the results

For study like LST retrieval from remotely sensed data, the most important thing is the validation of the results in order to confirm the appicability of the method and the accuracy of the work. In this case, the MODIS/Terra LST/Emissivity 5-min L2 Swath1km data was used to assess the accuracy of the work. The quick visualization of the map of MODIS/Terra LST/ Emissivity 2018 data shows the same areas with the same land surface temperature (urban areas with high temperature and other zones with less surface temperature) if compared with the computed land surface temperature, even though there are little difference between the values due probably to the time of image acquisition. The 1988 calculated LST was not validated unfortunately because of inexistence of the MODIS data. This absence is due to that MODIS begun to acquire LST/Emissivity data in the zone from the year 2000.

5 CONCLUSION

In this study, remote sensing and GIS were integrated for the evaluation of urban expansion and its impact on land surface temperature in Lomé city, Togo. Results showed a significant increase in urban LULC changes between 1988 and 2018 where most land covers such as vegetation and framlands were converted to urban or built-up with the highest LST all the times. In addition, it showed raise of the LST minimum from 12.76°C in 1988 to 22.76°C in 2018. The reasons could be either reduction in greenness or high surface radiation due to development of impervious surfaces. It can be concluded that rapid urbanization with high surface radiant covers is the most responsible of land surface temperature increase in urban areas.

Nowaday integration of remote sensing and GIS techniques showed its capabilities to detect urban expansion and then to evaluate its impact on environment. It allows for an examination of the impact factors of urban expansion on LST and then mitigate them through decision on planning. In this study, the increase of LST was highly related to the augmentation of high surface radiant covers and the decrease of biomass, indicating that urban expansion would be one of the main causes of temperature increase or global warming due to intense human activities and decision must be taken to mitigate the current situation.

REFERENCES

[1] Ustin, S. L., Roberts, D. A., Gamon, J. A., Asner, G. P. & Green, R. O., "Using imaging spectroscopy to study ecosystem processes and properties", Bioscience, 54, 523-534, 2004.

[2] Duan, S.-B., Li, Z.-L., Tang, B.-H., Wu, H. & Tang, R., "Generation of a time-consistent land surface temperature product from modis data", Remote sensing of environment, 140, 339-349, 2014.

[3] Ehlers, M. Et al., "Application of SPOT data for regional growth analysis and local planning", Photogrammetric Engineering and Remote Sensing, 56, 175–180, 1990.

[4] Jimenez-Munoz, J. C. et al., "Land surface temperature retrieval methods from Landsat-8 thermal infrared sensor data", Geoscience and remote sensing letters, IEEE, 11, 1840-1843, 2014.

[5] Jalili, S. Y., "The effect of land use on land surface temperature in the Netherlands", M.Sc, Lunds Universitet, Netherlands, 2013.

[6] Ahmed, B., Kamruzzaman, M., Zhu, X., Rahman, M.S., & Choi, K., "Simulating land cover changes and their impacts on land surface temperature in Dhaka", Bangladesh Remote Sensing, 5(11), 5969 – 5998, 2013.

[7] Mbithi DM, Demessie ET, Kashiri T., "The impact of Land Use Land Cover (LULC) Changes on Land Surface Temperature (LST); a case study of Addis Ababa City, Ethiopia", Kenya Meteorological Services, Laikipia Airbase, P.O. Box 192-10400 Nanyuki Town, Kenya, 2010.

[8] Mallick, J., Kant, Y. & Bharath, B., "Estimation of land surface temperature over Delhi using Landsat-7 ETM+", Journal Ind. Geophys. Union, 12, 131-140, 2008.

[9] Z. Wang et al., "Application of a normalized difference impervious index (NDII) to extract urban impervious surface features based on Landsat TM images", International Journal of Remote Sensing, vol. 36(4), pp. 1055-1069, 2015.

[10] Islam MS, Islam KS., "Application of thermal infrared remote sensing to explore the relationship between land use-land cover changes and urban heat Island effect: a case study of Khulna City", Journal Bangladesh Inst., Plan 6:49–60, 2013.

[11] Kumar KS et al., "Estimation of land surface temperature to study urban heat Island effect using Landsat ETM + Image", International Journal of Engineering Science and Technology, 4(2):771–778, 2012.

[12] Liu L, Zhang Y., "Urban heat Island analysis using the Landsat TM data and ASTER data: a case study in Hong Kong", Remote Sensing, 3:1535–1552. doi:10.3390/rs3071535, 2011.

[7] Lo, C. P., et al., "Application of high-resolution thermal infrared remote sensing and GIS to assess the urban heat island effect", International Journal of Remote Sensing, 18, 287–304, 1997.

[13] Sobrino, J. & Raissouni, N., "Toward remote sensing methods for land cover dynamic monitoring: application to Morocco", International journal of remote sensing, 21, 353-366, 2000.

[14] Rajeshwari A, Mani ND, "Estimation of land surface temperature of Dindigul district using Landsat 8 data", International Journal Resource Engineering and Technology, 3(5):122–126, 2014.

[15] Rozenstein O et al., "Derivation of land surface temperature for Landsat-8 TIRS using a split window algorithm", Sensors, 14:5768–5780. doi:10.3390/s140405768, 2014.

[16] Yeh, A. G. O., and Li, X., "Urban growth management in the Pear River delta—an integrated remote sensing and GIS approach" ITC Journal, 1, 77–85, 1996.

[17] Torrion, J. A., Maas, S. J., Guo, W., Bordovsky, J. P. & Cranmer, A. M., "A three-dimensional index for characterizing crop water stress", Remote sensing, 6, 4025-4042, 2014.

[18] Cammalleri, C. & Vogt, J., "On the role of land surface temperature as proxy of soil moisture status for drought monitoring in Europe", Remote sensing, 7, 16849-16864, 2015.

[19] Li, H.; Sun, D.; Yu, Y.; Wang, H.; Liu, Y.; Liu, Q.; Du, Y.; Wang, H.; Cao, B., "Evaluation of the VIIRS and MODIS LST products in an arid area of northwest China", Remote Sensing of Environment, 142, 111–121, 2014.

https://landsat.usgs.gov/using-usgs-landsat-8-product
https://earthexplorer.usgs.gov/